ACS OMEGA

Open Access

http://pubs.acs.org/journal/acsodf

Article

Wettability Characteristics of Low-Rank Coals Under the Coupling Effect of High Mineralization and Surfactants

Hongyong Liu, Zhen Li, Chunshan Zheng, Yushan Wang,* Fei Song, and Xiangfei Meng

Cite This: *ACS Omega* 2023, 8, 39004−39013

Read Online

ACCESS | Metrics & More | Article Recommendations

ABSTRACT: This paper investigates the unclear influence mechanism of the surfactant effect on improving coal seam wettability and CO_2-enhanced coalbed methane technology to enhance the gas extraction efficiency in some coal mines under highly mineralized environments in China. Specifically, the microinfluence mechanism of the coupling effect of nonionic surfactant OP-10 and highly mineralized coal samples under special treatment on the wettability of coal seam is examined. By measuring the contact angle and surface tension of the samples, it is confirmed that high mineralization can limit the effect of surfactants on improving the wettability of coal seams to a certain point. Infrared spectroscopy and X-ray diffraction measurements were conducted on the samples under coupling conditions. It is found that high mineralization impedes the effectiveness of surfactants in enhancing the wettability of coal seams. The surfactants interact with coal samples at the functional group level, producing new hydrophilic functional groups and increasing the content of kaolin with strong hydrophilic properties, thereby increasing the wettability of coal seams. However, these hydrophilic functional groups disappear under coupling conditions and hydrophobic functional groups are produced. Additionally, high mineralization inhibits the effect of surfactants on the phase composition of coal samples. The findings of this research provide a theoretical basis for water injection of highly mineralized coal seams and methane replacement recovery by carbon dioxide technology, promoting the practical application of water injection and gas injection displacement of coal seams.

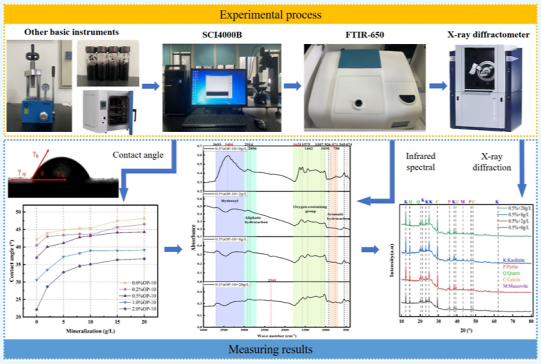

1. INTRODUCTION

China has abundant coal resources with considerable potential for development. On the other hand, these mines are characterized by intricate tectonics and late formation.[1−3] In cases where coal and gas outbursts occurred, injecting water into the coal seams proves an effective method for enhancing gas extraction rates in coal seams and resolving mine disasters.[4−7] The efficacy of water injection for gas extraction is directly proportional to the wettability of the coal seam. The hydrogeological conditions in the strata are intricate, with most coal seams located in areas with a high water content. Water content and mineralization remarkably affect the physical and chemical characteristics, permeability, and gas adsorption and desorption of coal.[8,9]

Experimental studies aimed at improving the wettability of coal seams and gas extraction efficiency concentrated on water injection and gas injection displacement. Research on water injection focused on the use of surfactants.[10−12] Surfactants are the main wetting agents in improving wettability, and surface tension is a key parameter for their effectiveness.[13−16] Jiang et al. found that OP-10 surfactant solutions had the best effect on improving coal wettability based on surface tension and contact angle measurements of different wetting agents.[17,18] Several studies have explored the effect of wetting agents in different proportions or combined with other materials to improve the wettability of coal seams.[14,19−21] For instance, Zou et al. added water-based SiO_2 nanofluids to the wetting agent solution and proposed a water injection method for coal seam improvement.[22,23] Molecular simulation software has been employed by some scholars to investigate the mechanism of surfactant effect on enhancing coal seam wettability.[16,24,25] In addition, the COMSOL simulation software was used to develop a coupled damage model during water injection to increase gas extraction rates.[26,27] Studies on gas injection displacement for improving gas extraction rates can be categorized into two types: using gases with strong adsorption capacity or gases that can break the dynamic balance of coal seam gas.[28−30] CO_2-enhanced coalbed methane (CO_2-ECBM) technology is essential to ensure energy security and achieve the "dual carbon" goal. This technology is crucial for achieving the low-carbon, clean, and efficient

Received: May 22, 2023
Accepted: September 28, 2023
Published: October 10, 2023

https://doi.org/10.1021/acsomega.3c03583
ACS Omega 2023, 8, 39004−39013

utilization of coal-based fossil energy. The CO_2-ECBM technology has been widely adopted to increase coalbed methane production using competitive displacement among gases and reduce carbon emissions.

Due to the complexity of the coal mining environment in China, scholars have researched how to improve the wettability of coal seams, considering the influence of environmental conditions and factors such as mineralization.[2,31−33] Wei and Ibrahim conducted separate experiments on the gas desorption and wettability of coal under different conditions. The former found that the mineralization degree hindered the improvement of coal wettability,[33] and the latter added that the hydrophobicity and CO_2 adsorption capacity on the coal surface increased with the increasing mineralization levels.[2] In summary, previous studies on coal wettability focused on the impact of either surfactants or mineralization without exploring the combined effects of both factors. In coalbed methane mining, it is crucial to consider multiple factors, including coal seam water and mineralization, when designing a mining scheme to enhance the collection efficiency and safety of coalbed methane. The coal mines in China typically have a mineralization range of 1−3 g/L and can reach up to 4 g/L in specific regions, such as the western plateau, Huanghuai plain, and most coastal coal mines in east China.[34,35] The highly mineralized coal seams require the injection of surfactant solutions to enhance wettability, yet the mechanism behind this process is still unclear. In this sense, it is significant to study the wettability characteristics of low-rank coal seams under the coupling conditions of high mineralization and surfactants and the methane replacement recovery by CO_2 in coal seams.

This paper investigates the effects of different concentrations of nonionic surfactant OP-10 on coal samples with varying mineralization levels. The coupling effect of surfactants and high mineralization on the wettability of coal samples is examined by measuring parameters such as the contact angle and surface tension of coal seams. Furthermore, the microscopic modification mechanism of the coal seam is explored using infrared spectroscopy and X-ray diffraction (XRD). The research findings can serve as a theoretical foundation for water injection in highly mineralized coal seams and an optimal design of coalbed methane mining schemes to enhance collection efficiency and safety during coalbed methane extraction. Furthermore, these results can facilitate the practical application of water and gas injection displacement methods in coal seams.

2. EXPERIMENTAL DESIGN

2.1. Preparation of Test Materials. Test coal samples, surfactants, and mineralized water were utilized. Specifically, coal samples were obtained from the Liangjia coal mine in the Longkou mining area, Yantai, Shandong Province. These samples are low in metamorphic degree with a coal seam thickness of 1.5−5.34 m. The mine is stable and mineable. The coal strata consist mainly of mudstone, claystone, carbonaceous mudstone, oil shale, coal, and sandstone. The industrial analysis of the coal samples is shown in Table 1.

Considering the current state of coal seam mineralization and the need for economic benefits, nonionic surfactant OP-10 (alkylphenol ethoxylates) was chosen, which exhibits excellent wetting properties and does not react with coal seam minerals or other additional substances, i.e., $C_{10}H_{21}O(CH_2CH_2-O)_{10}H$.[21,36] In this study, wetting agent solutions were prepared with varying mass fraction concentrations of 0.2, 0.5, 1.0, and 2.0%.

Table 1. Industrial Analysis Results of Coal Samples

coal sample name	M_{ad} (%)	A_{ad} (%)	V_{ad} (%)	V_{adf} (%)	FC_{ad} (%)
YT	6.61	15.34	29.09	37.27	48.96

In accordance with GB/T 19223-2015 "Classification of coal mine water", mine water containing a total dissolved solids concentration of 1000 mg/L or higher is classified as highly mineralized water. The dissolved solids in mine water can be further categorized into anions (Cl^-, SO_4^{2-}, and HCO_3^-) and cations (Na^+, Mg^{2+}, and Ca^{2+}).[37,38] To simulate the field conditions, an experiment was conducted using pure inorganic salts, such as NaCl, $CaSO_4$, and $CaCl_2$, mixed with Na^+/Ca^{2+} = 2:1 to create highly mineralized solutions. These solutions were prepared with varying concentrations of 2, 5, 8, 10, 15, and 20 g/L.

2.2. Experimental Methods. The instruments used in this test included SCI4000B automatic dynamic contact angle measuring instrument, DF-4B tablet press machine, electronic scale, drying oven, FTIR-650 Fourier transform infrared spectrometer, and X-ray diffractometer.

To determine the contact angle and surface tension, coal samples with particle sizes of 0.074−0.2 mm were selected from raw coal after being sieved by a sifter. Wetting agent solutions with mass fraction concentrations of 0.2, 0.5, 1.0, and 2.0% and highly mineralized solutions with concentrations of 2, 5, 8, 10, 15, and 20 g/L were used as test reagents. Test methods were conducted as follows:

I After the raw coal was treated by air-blast drying at 48 °C for 48 h, it was submerged and left for 48 h at a room temperature of 25 °C. The mass ratio of coal to the mineralized solution was 1:1. After air-drying treatment for 48 h, the experiment was carried out.

II A dried coal sample was obtained and pressed for 2 min under a constant pressure of 20 MPa using a DF-4B tablet machine to create standard samples with a diameter of 13 mm and a height of 2 mm. The droplet size was set to 2 μL, and the contact angle data of each group were measured using the SCI4000B automatic dynamic contact angle measuring instrument.

III The density of each test group was measured using an electronic scale and measuring tubes. The density of mineralized water was determined at 1.007 g/cm^3, and that of the surfactant was 0.970 g/cm^3. The surface tension was measured using the suspended drop method.

The functional group and phase compositions of coal samples were determined using infrared spectroscopy and XRD. Test methods were conducted as follows:

I The coal samples were subjected to high-mineralization treatment in accordance with the procedure mentioned earlier. Coal particles ranging from 0.074 to 0.2 mm were selected. The infrared spectrometer scanning range was set from 4000 to 400 cm^{-1}, with 32 scanning times and a resolution of 1.5 cm^{-1}.

II Next, 2 g of potassium bromide was ground thoroughly in a mortar to obtain a particle size below 325 mesh. A small amount of powdered potassium bromide was added to the DF-4B tablet press machine using a small medicine spoon and pressed for 1 min under a steady pressure of 15 MPa to make a translucent and crack-free background plate with a mass ratio of coal and potassium bromide of 1:200.

https://doi.org/10.1021/acsomega.3c03583
ACS Omega 2023, 8, 39004−39013

Table 2. Results of Contact Angle of Coal Sample after Surfactant Titration under High Mineralization

	contact angle for different concentrations of mineralized water (°)						
concentrations of OP-10 (%)	0	2	5	8	10	15	20
0.0	42.22	43.96	44.89	45.33	45.42	47.47	48.15
0.2	40.49	43.02	43.40	43.73	43.54	45.65	46.50
0.5	36.99	40.07	41.14	42.80	43.20	44.15	44.30
1.0	30.57	33.49	37.20	38.21	38.94	38.96	39.15
2.0	22.13	28.68	32.79	34.55	35.08	36.36	36.63

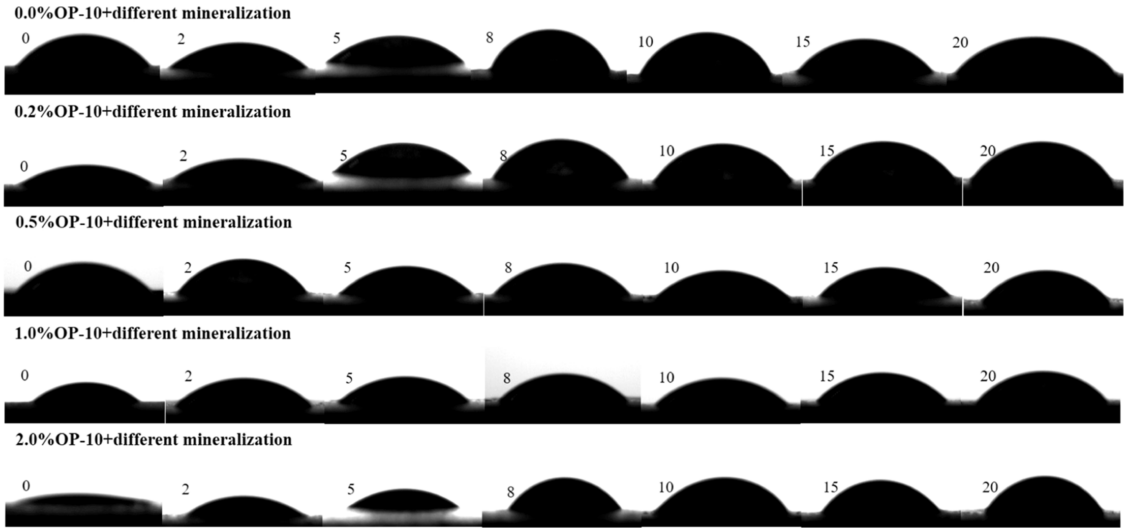

Figure 1. Contact angle diagram of coal samples.

To obtain the infrared spectral curves, the background plate was measured first, followed by the test plate using an FTIR-650 Fourier transform infrared spectrometer.

III The coal samples were treated with high mineralization following the instructions in Experiment 1. The samples were then ground to 325 mesh using a mortar and pestle. The X-ray diffractometer was set to scan at steps of 0.02°, with a scanning angle of 10−80° and a scanning time of 0.1 s.

IV The coal samples were placed in the slide groove using a medicine spoon. The slide was taken, the surface of each sample was lightly pressed, and samples beyond the groove were scraped off. After closing the door of the sample chamber, the test was commenced.

3. RESULTS AND DISCUSSION

3.1. Contact Angle Variation Pattern. The contact angle and the surface tension of coal samples satisfy the Young-equation relationship shown in (eq 1).[39,40]

$$\cos\theta = \frac{\gamma_{sg} - \gamma_{sl}}{\gamma_{lg}} \quad (1)$$

where θ is the three-phase contact angle, °; γ_{sg} is the solid−gas phase surface tension, mN/m; γ_{sl} is the solid−liquid phase surface tension, mN/m; and γ_{lg} is the liquid−gas phase surface tension, mN/m.

The contact angle measurement of the original coal samples with distilled water is 42.22°, indicating that it is hydrophilic. The contact angle measurements under different coupling conditions are listed in Table 2. The contact angle of coal samples elevates with an increase in mineralization degree at any given surfactant concentration, suggesting that mineralization degree has an inhibitory effect on the wettability of coal samples. The inhibitory effect is observed with a range of 14.05−65.52% and becomes notable with the surfactant concentrations. The contact angle measurement diagram is shown in Figure 1.

The contact angle data were plotted as a curve illustrated in Figure 2. It is evident that the rate of change of the contact angle decreases with an increase in mineralization, and the concentration of OP-10 remains constant. The average change rate decreases significantly from 1.682°/(g/L) to 0.0856°/(g/L), indicating a limited value for its inhibitory effect.

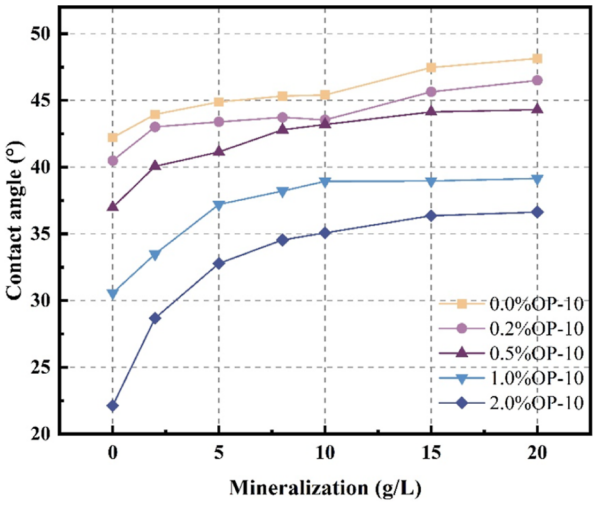

Figure 2. Contact angle change curve under coupling condition.

https://doi.org/10.1021/acsomega.3c03583
ACS Omega 2023, 8, 39004−39013

3.2. Surface Tension Variation Pattern. According to Table 3, the surface tension of the solution decreases rapidly upon adding OP-10. The mineralized solution shows a slight increase in surface tension, indicating that mineralization still has an inhibitory effect on the wettability of coal samples in terms of surface tension.

Table 3. Determination Results of Surface Tension of Each Concentration Test Reagent

concentrations of OP-10 (%)	0	0.2	0.5	1.0	2.0
surface tension (mN/m)	73.40	33.727	32.485	31.914	31.241
mineralization (g/L)	2	5	8	15	20
surface tension (mN/m)	73.518	73.587	73.614	73.704	73.913

The surface tension data are presented as a curve in Figure 3. The results indicate that the surfactant decreases the surface tension of the solution by 57.4%, as demonstrated by a sharp downward trend in the graph. When the mineralization increases, the surface tension of the solution shows a gradual increase with a maximum change of 0.72%. Both solutions exhibit a gentle changing trend with increasing concentrations, suggesting a limit to the influence of the two solutions on the surface tension.

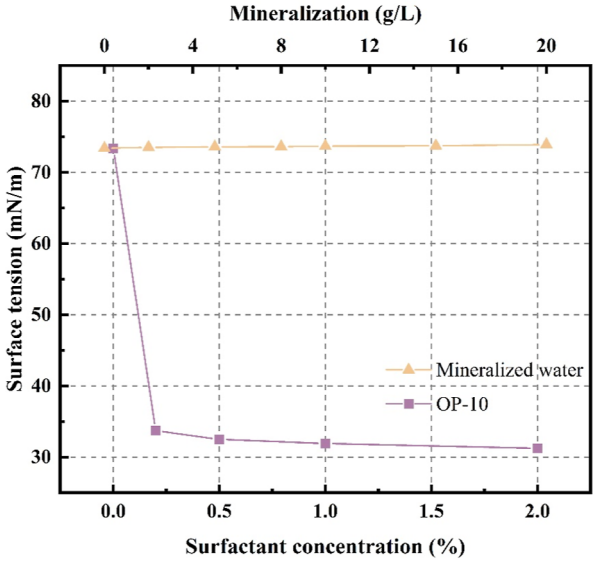

Figure 3. Variation curve of surface tension.

The results of contact angle and surface tension measurements suggest that high mineralization coupling to surfactants limits the effectiveness of the surfactants. There appears to be a threshold for this inhibitory effect, and further analysis of the microscopic mechanism by which mineralization affects coal seam wettability is needed

3.3. Analysis of Infrared Spectral Measurements. The infrared spectral measurements were analyzed by considering pure surfactant treatment and coupling treatment with high mineralization, displayed in Figures 4 and 5, respectively. The types and quantities of the functional groups in the coal samples were determined by analyzing the positions, intensities, and vibration patterns of different absorption peaks in the infrared spectrograms.

The absorption region of the hydroxyl (−OH) functional group is between the wavenumbers 3000 and 3700 cm^{-1}, as indicated by Figure 4. The absorption peaks are primarily observed at 3693 and 3404 cm^{-1}, resulting from the −OH stretching vibration. When exposed to infrared light, the untreated OP-10 coal samples do not exhibit any absorption peaks at 3404 cm^{-1}, indicating the emergence of new −OH structures in the OP-10-treated coal samples. This also suggests the formation of new hydrogen bonds in the treated samples, enhancing wettability. These findings align with the contact angle and surface tension analysis results discussed in the previous section. The intensity of the absorption peak tends to increase with the surfactant concentrations, which is consistent with Lambert's law that the absorbance is proportional to the concentration of the sample.[41] Additionally, the −OH vibrations at 3924 and 3820 cm^{-1} are caused by the presence of inadequately dried water in the test samples.

The absorption region of the aliphatic structure lies between 2700 and 3000 cm^{-1}. This region is primarily composed of methyl2013CH_3 and methylene-CH_2, with two absorption peaks appearing at 2914 and 2856 cm^{-1}, caused by the asymmetric and symmetric stretching vibrations of the two components. The intensity of the absorption peaks in this band is low, and their relationship with the surfactant concentration is not significant.

In the range of 1000−1800 cm^{-1}, it is the absorption region of oxygen-containing functional groups, including carbonyl C═O, carboxyl −COOH, ester −COOR, etc. More absorption peaks are observed in this region, such as aldehyde and ketone C═O stretching vibration at 1710 cm^{-1}, amide C═O stretching vibration at 1628 and 1575 cm^{-1}, alcohol and phenol −OH bending vibration at 1442 and 1346 cm^{-1}, alcohol and phenol C═O stretching vibration at 1107 and 1030 cm^{-1}, and ether antisymmetric stretching vibration at 1246 cm^{-1}. An absorption peak is presented at 1710 cm^{-1} in the infrared spectrogram of the untreated coal samples, generated by the C═O stretching vibration, and disappears with the increase of OP-10 concentration. Two new absorption peaks are generated at 1346 and 1246 cm^{-1} under the OP-10 concentrations of 1.0 and 2.0% in the treated coal samples, indicating that new oxygen-containing functional groups are created and the wettability of coal samples is enhanced due to the surfactant treatment.

The absorption region of the aromatic structural functional groups ranges from 700 to 900 cm^{-1}. It mainly comprises the olefin CH═CH bending vibration at 926 cm^{-1}, 1,4-disubstituted benzene at 871 cm^{-1}, and monosubstituted benzene at 758 cm^{-1}, with three absorption peaks. These functional groups are hydrophobic functional groups. Two absorption peaks appear at 545 and 474 cm^{-1}, produced by the vibrations of the halides of Cl, Br, and I.

The results from Figure 5 indicate two absorption peaks generated by −OH stretching vibration within the wavenumber range of 3000−3700 cm^{-1}, specifically at 3693 and 3404 cm^{-1}. However, the broad absorption peak of −OH at 3404 cm^{-1} disappears after the addition of mineralized water, suggesting that the weakened wettability of the coal samples by mineralized water treatment is attributed to the addition of mineralized molecules that destroy some −OH functional groups.

From 2700 to 3000 cm^{-1}, two absorption peaks between 2914 and 2856 cm^{-1} are generated by the asymmetric and symmetric stretching vibrations of methyl and methylene. Notably, a new absorption peak appears in the infrared spectrogram of the coal samples under the coupling treatment of 0.5% OP-10 and 20 g/

https://doi.org/10.1021/acsomega.3c03583
ACS Omega 2023, 8, 39004−39013

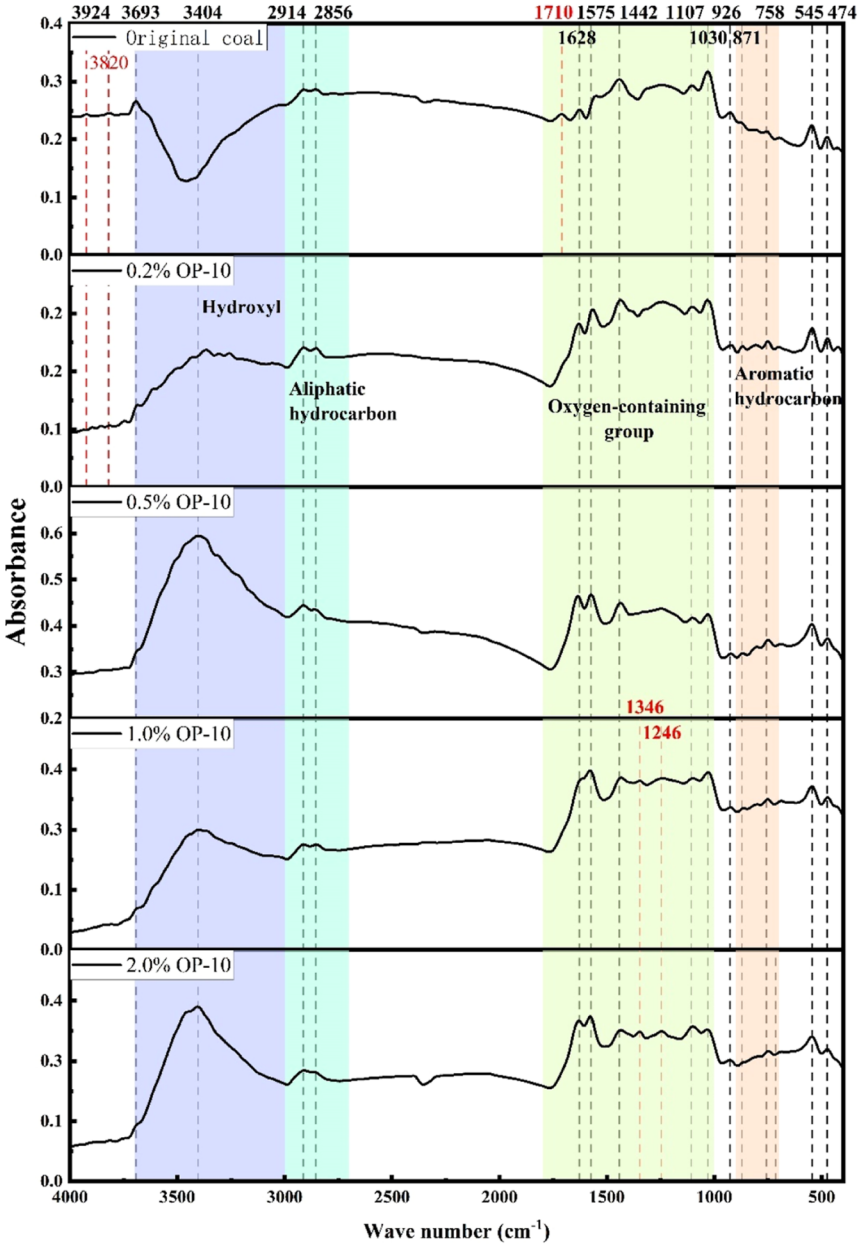

Figure 4. Infrared spectra of coal samples treated with surfactants at varying concentrations.

L mineralized water, and its intensity and width are relatively small, at 2341 cm^{-1}. It is possibly attributed to the stretching vibration of C═C, which is correlated with the mineralization concentration.

In the range from 1000 to 1800 cm^{-1}, absorption peaks at 1628, 1575, 1442, 1107, and 1030 cm^{-1} are observed. However, the absorption peak at 1628 cm^{-1} generated by the C═O stretching vibration disappears when mineralized water is added to the coupling.

The absorption peaks at 926, 871, and 758 cm^{-1} remain unchanged in the range of 700−900 cm^{-1}. The absorption peak at 871 cm^{-1}, which belongs to 1,4-disubstituted benzene, disappears and is no longer reflected at 2 g/L mineralization. The number and intensity of the halogen absorption peaks at 545 and 474 cm^{-1} remain unaffected.

The surfactant OP-10 increases the wettability of coal seams by creating new hydrophilic oxygen-containing functional groups at wave numbers of 3693 and 3404 cm^{-1}. The addition of highly mineralized water eliminates these groups at 3404 and 1628 cm^{-1} and generates new hydrophobic functional groups at 2341 cm^{-1}, decreasing the wettability of coal samples.

3.4. Analysis of XRD Measurement Results. The XRD results were analyzed with regard to pure surfactant treatment and high mineralization coupling. The measured curves were compared to the standard PDF card. The XRD measurements under pure surfactant and coupling conditions are shown in Figures 6 and 6, respectively.

According to Figure 6, coal primarily contains mineral elements such as K, Al, Mg, Fe, and Ca, and others such as S, Si, C, etc. The predominant inferred compositions are mainly kaolinite $Al_4[SiO_4O_{10}](OH)_8$, calcite $CaCO_3$, quartz SiO_2, pyrite FS_2, muscovite Ca $Mg(CO_3)_2$, etc. The concentration of surfactants has few impacts on the physical composition and phase content of the coal samples. The highest content of the samples is kaolinite, followed by quartz, calcite, pyrite, and muscovite contribute to the lowest content.

https://doi.org/10.1021/acsomega.3c03583
ACS Omega 2023, 8, 39004−39013

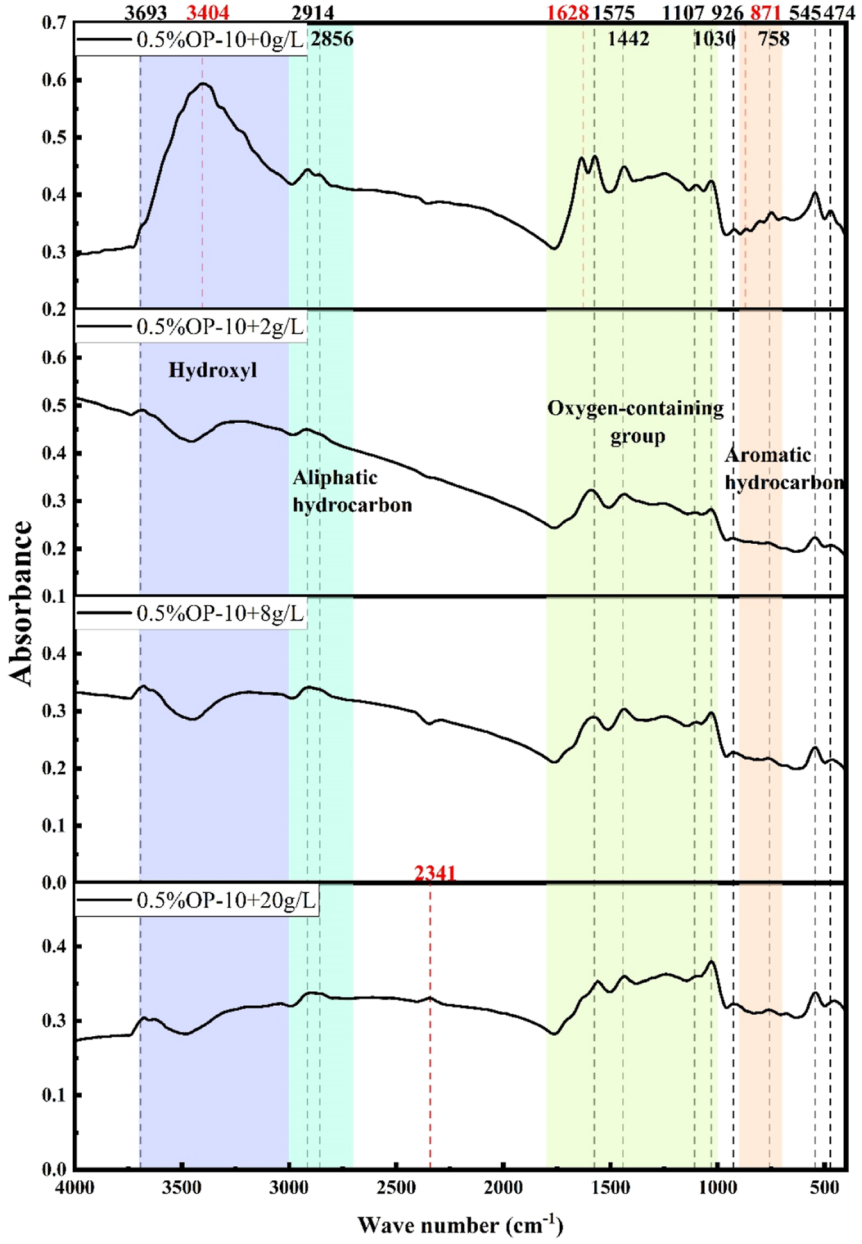

Figure 5. Infrared spectra of coal samples under the coupling of 0.5% OP-10 and different mineralization.

The quantitative analysis of the XRD patterns of the composition is presented in Table 4. Consistent with the results in Figure 6, the component ranking is as follows: kaolinite (~50%) > quartz (~30%) > calcite (~15%) > pyrite and muscovite (~10% or less). A significant increase in kaolinite content is seen with the surfactant concentrations, from 45.7% at untreated conditions to 54.9% treated with a concentration of 2.0% OP-10. Conversely, the quartz content decreases from 31.9 to 23.3% with the addition of P-10. The contents of the other three minerals remain relatively stable throughout the experiment. Kaolinite, a clay mineral, exhibits stronger hydrophilicity compared to quartz minerals.[42,43] This explains why surfactants improve the wettability of coal seams at the phase composition level.

The results in Figure 7 demonstrate that the phase composition and distribution of coal samples coupled with high mineralization are consistent with those of pure surfactants, suggesting that the concentration of mineralization does not significantly impact the phase composition of coal samples. Nevertheless, they inhibit the influence of surfactants on the phase composition of coal samples. The phase composition of coal samples under coupling conditions is quantitatively analyzed, and the results are summarized in Table 5.

According to Table 5, the content of each mineral fluctuates slightly with changes in the concentration of the mineralized water. This changing rule differs from that of samples with pure surfactants. The addition of high mineralization inhibits the effect of surfactants on the phase composition of coal samples. Each component fluctuates within an average range.

In terms of the coal sample phase composition, the use of surfactant OP-10 increases the content of kaolinite which is more hydrophilic, thereby improving the wettability of the coal seam. In contrast, the addition of highly mineralized water counteracts this effect, inhibiting the effect of the surfactant on the phase composition of the coal samples. Ultimately, this reversal of the effect reduced the wettability of the coal seam.

https://doi.org/10.1021/acsomega.3c03583
ACS Omega 2023, 8, 39004−39013

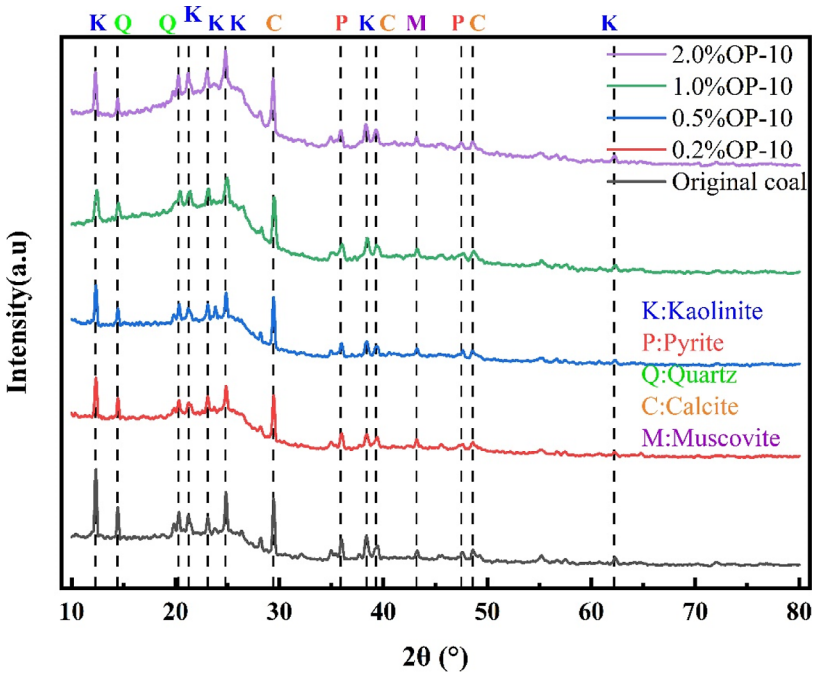

Figure 6. X-ray diffraction patterns of coal samples treated with surfactants of different concentrations.

Table 4. Determination Results of Mineral Content of Coal Samples under Surfactant Treatment

	mineral content (%)				
concentrations of OP-10 (%)	kaolinite (%)	pyrite (%)	quartz (%)	calcite (%)	muscovite (%)
original coal	45.7	5.1	31.9	14.1	3.2
0.2%	48.5	4.5	30.1	13.8	3.0
0.5%	49.3	4.5	27.5	15.7	2.9
1.0%	47.9	5.2	30.9	12.7	3.3
2.0%	54.9	4.4	23.3	14.7	2.8

Table 5. Determination Results of Mineral Content of Coal Samples under Coupling Treatment

	mineral content (%)				
mineralization (g/L)	kaolinite (%)	pyrite (%)	quartz (%)	calcite (%)	muscovite (%)
0.5% + 0	49.3	4.5	27.5	15.7	2.9
0.5% + 2	51.0	3.6	26.5	16.3	2.6
0.5% + 8	50.1	3.6	32.2	11.5	2.5
0.5% + 20	49.9	3.3	31.0	13.4	2.4

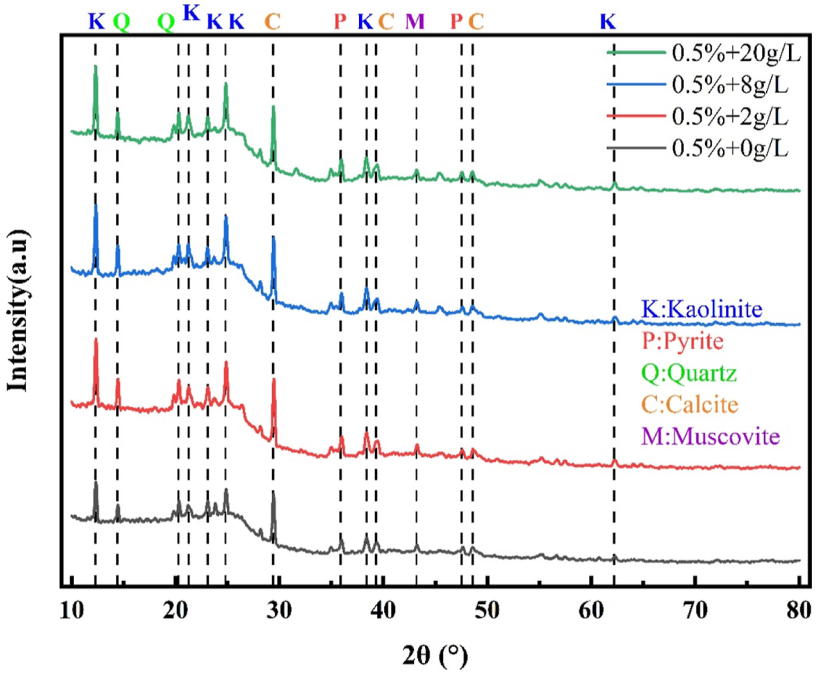

Figure 7. X-ray diffraction pattern of coal samples under the coupling of 0.5% OP-10 and different mineralization.

https://doi.org/10.1021/acsomega.3c03583
ACS Omega 2023, 8, 39004−39013

3.5. Analysis of the Mechanism of Surfactant Effect on Coal Wettability under High Mineralization. This study investigates the coal seam wettability under coupling conditions of high mineralization and surfactants. The contact angle of coal samples and the surface tension of experimental reagents with different concentrations were measured to determine the direction of effect. The results indicate that the addition of high mineralization inhibits the effect of surfactant OP-10 on the contact angle and surface tension of the coal samples. Increasing the contact angle and surface tension reduces the wettability of the coal seams. The microinfluence mechanism of high mineralization and surfactants on the wettability of coal seams from the perspective of microfunctional group and phase compositions is examined. An increase in the surfactant concentration produces new hydrophilic oxygen-containing functional groups in the −OH absorption zone. Additionally, the content of kaolin with increasing hydrophilicity also increases, which enhances the wettability of the surfactant-treated coal samples. High mineralization levels destroy hydrophilic functional groups, specifically the −OH and oxygen-containing functional groups, and absorption peaks of the hydrophobic functional group C═C emerge. In addition, the effect of surfactants on the phase composition of coal samples is inhibited with the addition of high mineralization, thus reducing the wettability of coal seams.

It is found that the ability to enhance the wettability of the coal seam under the combined effect of high mineralization and surfactant is weaker than that under pure surfactant conditions. This is because the addition of high-mineralization conditions destroys the original hydrophilic functional groups and generates new hydrophobic functional groups of the coal sample. The presence of these hydrophobic groups reduces the wettability of the coal seam. After the addition of high mineralization conditions to the original surfactant, the surfactant-induced change in phase content of coal samples is no longer evident. Instead, each component fluctuates within an average value range, inhibiting the effect of surfactant on the phase composition of the coal samples and ultimately reducing the wettability of the coal seam.

4. CONCLUSIONS

This study examines the coupling effect of high mineralization and surfactants on the wettability of coal seams by analyzing the contact angle, actual surface tension, functional group composition, and phase composition of the coal samples. The results provide valuable data for the practice and research of CO_2-ECBM engineering in China. The main conclusions are as follows:

1 The high mineralization in coal seams hinders the effectiveness of surfactants in improving wettability. This inhibitory effect is demonstrated by an increase in the contact angle and surface tension of coal samples with an upper limit.

2 When pure surfactants are applied, hydrophilic functional groups emerge at 3693 and 3404 cm^{-1}, accompanied by an increase in kaolin content. Under coupling conditions, hydrophilic functional groups disappear at 3404 and 1628 $cm^{-1,}$ and hydrophobic functional groups emerge at 2341 cm^{-1}. The high mineralization level inhibits the effect of surfactants on the phase composition of coal samples.

3 This study explores the microinfluence mechanism of high mineralization and surfactants on the wettability of coal seams. The addition of high mineralization destroys hydrophilic functional groups and generates new hydrophobic functional groups, ultimately reducing the wettability of coal seams. Additionally, surfactants have an inhibitory effect on the phase composition of coal samples.

AUTHOR INFORMATION

Corresponding Author

Yushan Wang − *Key Laboratory of Coal Mine Gas and Fire Prevention, Ministry of Education, China University of Mining and Technology, Xuzhou 221116 Jiangsu, China; School of Safety Engineering, China University of Mining and Technology, Xuzhou 221116 Jiangsu, China;* orcid.org/0000-0003-1013-1621; Email: TS21120155P31@cumt.edu.cn

Authors

Hongyong Liu − *Institute of Energy, Hefei Comprehensive National Science Center (Anhui Energy Laboratory), Hefei 230031 Anhui, China; Key Laboratory of Coal Mine Gas and Fire Prevention, Ministry of Education, China University of Mining and Technology, Xuzhou 221116 Jiangsu, China; School of Safety Engineering, China University of Mining and Technology, Xuzhou 221116 Jiangsu, China*

Zhen Li − *Key Laboratory of Coal Mine Gas and Fire Prevention, Ministry of Education, China University of Mining and Technology, Xuzhou 221116 Jiangsu, China; School of Safety Engineering, China University of Mining and Technology, Xuzhou 221116 Jiangsu, China*

Chunshan Zheng − *Institute of Energy, Hefei Comprehensive National Science Center (Anhui Energy Laboratory), Hefei 230031 Anhui, China; School of Safety Science and Engineering, Anhui University of Science and Technology, Huainan 232001 Anhui, China;* orcid.org/0000-0003-0255-6005

Fei Song − *Key Laboratory of Coal Mine Gas and Fire Prevention, Ministry of Education, China University of Mining and Technology, Xuzhou 221116 Jiangsu, China; School of Safety Engineering, China University of Mining and Technology, Xuzhou 221116 Jiangsu, China*

Xiangfei Meng − *Key Laboratory of Coal Mine Gas and Fire Prevention, Ministry of Education, China University of Mining and Technology, Xuzhou 221116 Jiangsu, China; School of Safety Engineering, China University of Mining and Technology, Xuzhou 221116 Jiangsu, China*

Complete contact information is available at: https://pubs.acs.org/10.1021/acsomega.3c03583

Notes

The authors declare no competing financial interest.

ACKNOWLEDGMENTS

This work is supported by the University Synergy Innovation Program of Anhui Province no. GXXT-2021-018, the Fundamental Research Funds for the Central Universities no. 2020ZDPYMS13, the Institute of Energy, Hefei Comprehensive National Science Center under grant no. 21KZS218, the Independent Innovation Project of Double First-class Construction of China University of Mining and Technology no. 2022ZZCX05K02.

https://doi.org/10.1021/acsomega.3c03583
ACS Omega 2023, 8, 39004−39013

REFERENCES

(1) Tang, Y.; Wang, X.; Schobert, H. H.; Eble, C. F.; Yang, C.; Su, Y.; Ye, K.; Cao, Q.; Liu, G. Cleaning Potential of Selected Coals in Shanxi Province, China: Evaluation of Geological Factors Affecting the Cleaning Potential. *Energy Fuels* **2020**, *34*, 1396−1407.

(2) Ibrahim, A. F.; Nasr-El-Din, H. A. Effect of Water Salinity on Coal Wettability During CO2 Sequestration in Coal Seams. *Energy Fuels* **2016**, *30*, 7532−7542.

(3) Yu, C.; Mu, N.; Huang, W.; Xu, W.; Feng, X. Major and Rare Earth Element Characteristics of Late Paleozoic Coal in the Southeastern Qinshui Basin: Implications for Depositional Environments and Provenance. *ACS Omega* **2022**, *7*, 30856−30878.

(4) Yan, J.; Wang, F.; Li, Y.; Gao, Y.; Li, Z.; Liu, H. A Feasibility Study of Coal Seam Water Injection Processes: The Effects of Coal Porosity and Mass Flow Rates of Injected Water on Wetting Radii. *Energy Fuels* **2020**, *34*, 16956−16967.

(5) Chen, Y.; Chu, T.; Chen, X.; Chen, P. Comparative Analysis of Gas-Solid-Liquid Coupling Behavior in Front of the Working Face Before and After Water Injection During Coal Mining. *Nat. Resour. Res.* **2021**, *30*, 1561−1575.

(6) Wang, G.; Liu, Y.; Huang, Q.; Wang, E.; Liu, N. Experimental Study on the Influence of Coal Fracture Surface Roughness on Water Injection Seepage. *ACS Omega* **2022**, *7*, 32679−32689.

(7) Xiao, Z.; Shi, Q.; Zhang, X. Influence of High-Pressure Water Injection on the Pore Structure of Anthracite Coal in Xinjing Coal Mine. *ACS Omega* **2021**, *6*, 148−158.

(8) Li, J.; Wang, Y.; Chen, Z.; Rahman, S. S. Effects of moisture, salinity and ethane on the competitive adsorption mechanisms of CH_4/CO_2 with applications to coalbed reservoirs: A molecular simulation study[J]. *J. Nat. Gas Sci. Eng.* **2021**, *95*, 104151.

(9) Ibrahim, A. F.; Nasr-El-Din, H. A. Effect of Water Salinity on Coal Wettability During CO_2 Sequestration in Coal Seams[J]. *Energy Fuels* **2016**, *30* (9), 7532−7542.

(10) Zhou, L.; Feng, Q. Y.; Chen, Z. W.; Liu, J. S. *2011 International Conference of Environmental Science and Engineering, vol 12, PT B*; Ma, M., Ed.; International Conference on Environment Science and Engineering (ICESE), 2012; Vol. *12*.

(11) Li, Z. W.; Yu, H. J.; Bai, Y. S. Numerical Simulation of CO2-ECBM Based on Multi-Physical Field Coupling Model. *Sustainability* **2022**, *14*, 11789.

(12) Ameri, A.; Kaveh, N. S.; Rudolph, E. S. J.; Wolf, K. H.; Farajzadeh, R.; Bruining, J. Investigation on Interfacial Interactions among Crude Oil-Brine-Sandstone Rock-CO2 by Contact Angle Measurements. *Energy Fuels* **2013**, *27*, 1015−1025.

(13) Le, T. T. Y.; Tsay, R.; Lin, S. A study on the dynamic surface tension of surfactant solutions at dilute concentrations. *J. Mol. Liq.* **2021**, *324*, 115112.

(14) Wang, K.; Ma, X.; Jiang, S.; Wu, Z.; Shao, H.; Pei, X. Application study on complex wetting agent for dust-proof after gas drainage by outburst seams in coal mines. *Int. J. Min. Sci. Technol.* **2016**, *26*, 669−675.

(15) Yuan, M.; Nie, W.; Zhou, W.; Yan, J.; Bao, Q.; Guo, C.; Tong, P.; Zhang, H.; Guo, L. Determining the effect of the non-ionic surfactant AEO9 on lignite adsorption and wetting via molecular dynamics (MD) simulation and experiment comparisons. *Fuel* **2020**, *278*, 118339.

(16) Sun, L.; Ge, S.; Jing, D.; Liu, S.; Chen, X. Wetting Mechanism and Experimental Study of Synergistic Wetting of Bituminous Coal with SDS and APG1214. *ACS Omega* **2022**, *7*, 780−785.

(17) Liao, X.; Wang, B.; Wang, L.; Zhu, J.; Chu, P.; Zhu, Z.; Zheng, S. Experimental Study on the Wettability of Coal with Different Metamorphism Treated by Surfactants for Coal Dust Control. *ACS Omega* **2021**, *6*, 21925−21938.

(18) Jiang, Y.; Wang, P.; Liu, R.; Pei, Y.; Wu, G.; Aizenshtein, M. An Experimental Study on Wetting of Coal Dust by Surfactant Solution. *Adv. Mater. Sci. Eng.* **2020**, *2020*, 1−13.

(19) Wang, Y.; Yang, W.; Li, Y.; Liu, T.; Si, G.; Luo, L. Effect of SDS modified coal microstructure on wettability and methane adsorption. *Fuel* **2023**, *337*, 127174.

(20) Zhang, T.; Zou, Q.; Li, K.; Jia, X.; Jiang, C.; Niu, X. Effect of SiO2 nanofluid with different concentrations on the wettability of coal. *Fuel* **2022**, *321*, 124041.

(21) Wang, P.; Jiang, Y.; Liu, R.; Liu, L.; He, Y. Experimental study on the improvement of wetting performance of OP-10 solution by inorganic salt additives. *Atmos. Pollut. Res.* **2020**, *11*, 153−161.

(22) Xu, J.; Zhang, Y.; Chen, H.; Wang, P.; Xie, Z.; Yao, Y.; Yan, Y.; Zhang, J. Effect of surfactant headgroups on the oil/water interface: An interfacial tension measurement and simulation study. *J. Mol. Struct.* **2013**, *1052*, 50−56.

(23) Zou, Q.; Zhang, T.; Ma, T.; Tian, S.; Jia, X.; Jiang, Z. Effect of water-based SiO2 nanofluid on surface wettability of raw coal. *Energy* **2022**, *254*, 124228.

(24) Zhang, X.; Cheng, J.; Kang, T.; Zhou, X.; Zhang, L. Electrochemical Modification on CH(4) and H(2)O Wettability of Qinshui Anthracite Coal: A Combined Experimental and Molecular Dynamics Simulation Study. *ACS Omega* **2021**, *6*, 24147−24155.

(25) Sun, L.; Ge, S.; Liu, S.; Jing, D.; Chen, X. Experimental and Molecular Dynamics Simulation Study for Preferring Coal Dust Wetting Agents. *ACS Omega* **2022**, *7*, 17593−17599.

(26) Chen, Y.; Xu, J.; Peng, S.; Yan, F.; Fan, C. A Gas-Solid-Liquid Coupling Model of Coal Seams and the Optimization of Gas Drainage Boreholes. *Energies* **2018**, *11*, 560.

(27) Shao, J.; Zhang, W.; Wu, X.; Lei, Y.; Wu, X. Rock Damage Model Coupled Stress-Seepage and Its Application in Water Inrush from Faults in Coal Mines. *ACS Omega* **2022**, *7*, 13604−13614.

(28) Fan, C.; Yang, L.; Wang, G.; Huang, Q.; Fu, X.; Wen, H. Investigation on Coal Skeleton Deformation in CO2 Injection Enhanced CH4 Drainage From Underground Coal Seam. *Front. Earth Sci.* **2021**, *9*, 766011..

(29) Ren, T.; Wang, G.; Cheng, Y.; Qi, Q. Model development and simulation study of the feasibility of enhancing gas drainage efficiency through nitrogen injection. *Fuel* **2017**, *194*, 406−422.

(30) Gong, H.; Wang, K.; Wang, G.; Yang, X.; Du, F. Underground coal seam gas displacement by injecting nitrogen: Field test and effect prediction. *Fuel* **2021**, *306*, 121646.

(31) Busch, A.; Krooss, B.; Gensterblum, Y.; van Bergen, F.; Pagnier, H. J. M. High-pressure adsorption of methane, carbon dioxide and their mixtures on coals with a special focus on the preferential sorption behaviour. *J. Geochem. Explor.* **2003**, *78*−*79*, 671−674.

(32) Zhang, S.; Liu, Y.; Meng, T. Experimental study on influence of water with different salinity on methane desorption performance of coal seam. *Coal Sci. Technol.* **2021**, *49*, 110−117.

(33) Wei, Y. C.; Xiang, X. X.; Wang, A. M.; Zhang, Q.; Cao, D. Y. Influence of water with different salinity on the adsorption performance of coal reservoir. *J. China Coal Soc.* **2019**, *44* (9), 2833−2839.

(34) Zhang, B.; Cheng, W.; Zhang, Q.; Li, Y.; Sun, P.; Fathy, D. Occurrence Patterns and Enrichment Influencing Factors of Trace Elements in Paleogene Coal in the Fushun Basin, China. *ACS Earth Space Chem.* **2022**, *6*, 3031−3042.

(35) Banks, E. W.; Smith, S. D.; Hatch, M.; Burk, L.; Suckow, A. Sampling Dissolved Gases in Groundwater at in Situ Pressure: A Simple Method for Reducing Uncertainty in Hydrogeological Studies of Coal Seam Gas Exploration. *Environ. Sci. Technol. Lett.* **2017**, *4*, 535−539.

(36) Shen, Y.; Li, Y.; Yao, Y.; Xia, Y.; Jiao, M.; Han, E. Electrodeposition and Catalytic Performance of Hydrophobic PbO2 Electrode Modified by Surfactant OP-10. *ECS J. Solid State Sci. Technol.* **2021**, *10*, 123005.

(37) Kumar, S.; Mandal, A. Studies on interfacial behavior and wettability change phenomena by ionic and nonionic surfactants in presence of alkalis and salt for enhanced oil recovery. *Appl. Surf. Sci.* **2016**, *372*, 42−51.

(38) Tang, H.; Zhao, L.; Sun, W.; Hu, Y.; Han, H. Surface characteristics and wettability enhancement of respirable sintering dust by nonionic surfactant. *Colloids Surf., A* **2016**, *509*, 323−333.

(39) Arif, M.; Jones, F.; Barifcani, A.; Iglauer, S. Influence of surface chemistry on interfacial properties of low to high rank coal seams. *Fuel* **2017**, *194*, 211−221.

https://doi.org/10.1021/acsomega.3c03583
ACS Omega 2023, 8, 39004−39013

(40) Young, T. An Essay on the Cohesion of Fluids. *Philos. Trans. R. Soc. London* **1805**, *95*, 65−87.
(41) Reis, R. L.; Filho, D. A. D. S. The effect of positional disorder and the Beer-Lambert law in organic photovoltaics. *J. Mol. Model.* **2022**, *28*, 330.
(42) Li, Y.; Xia, W.; Wen, B.; Xie, G. Filtration and dewatering of the mixture of quartz and kaolinite in different proportions. *J. Colloid Interface Sci.* **2019**, *555*, 731−739.
(43) Zhou, C.; Liu, L.; Chen, J.; Min, F.; Lu, F. Study on the influence of particle size on the flotation separation of kaolinite and quartz. *Powder Technol.* **2022**, *408*, 117747.

https://doi.org/10.1021/acsomega.3c03583
ACS Omega 2023, 8, 39004−39013